

Observation of interference between resonant and detuned STIRAP in the adiabatic creation of $^{23}\text{Na}^{40}\text{K}$ molecules

Lan Liu^{*,1,2} De-Chao Zhang^{*,1,2} Huan Yang,^{1,2} Ya-Xiong Liu,^{1,2} Jue Nan,^{1,2} Jun Rui,^{1,2} Bo Zhao,^{1,2} and Jian-Wei Pan^{1,2}

¹*Hefei National Laboratory for Physical Sciences at Microscale and Department of Modern Physics, University of Science and Technology of China, Hefei, Anhui 230026, China*

²*Shanghai Branch, CAS Center for Excellence and Synergetic Innovation Center in Quantum Information and Quantum Physics, University of Science and Technology of China, Shanghai 201315, China*

Stimulated Raman adiabatic passage (STIRAP) allows to efficiently transferring the populations between two discrete quantum states and has been used to prepare molecules in their rovibrational ground state. In realistic molecules, a well-resolved intermediate state is usually selected to implement the resonant STIRAP. Due to the complex molecular level structures, the detuned STIRAP always coexists with the resonant STIRAP and may cause unexpected interference phenomenon. However, it is generally accepted that the detuned STIRAP can be neglected if compared with the resonant STIRAP. Here we report on the first observation of interference between the resonant and detuned STIRAP in the adiabatic creation of $^{23}\text{Na}^{40}\text{K}$ ground-state molecules. The interference is identified by observing that the number of Feshbach molecules after a round-trip STIRAP oscillates as a function of the hold time, with a visibility of about 90%. This occurs even if the intermediate excited states are well resolved, and the single-photon detuning of the detuned STIRAP is about one order of magnitude larger than the linewidth of the excited state and the Rabi frequencies of the STIRAP lasers. Moreover, the observed interference indicates that if more than one hyperfine level of the ground state is populated, the STIRAP prepares a coherent superposition state among them, but not an incoherent mixed state. Further, the purity of the hyperfine levels of the created ground state can be quantitatively determined by the visibility of the oscillation.

Ultracold polar molecules offer great opportunities to study ultracold chemistry [1–4], quantum simulation [5, 6], quantum computation [7, 8] and to perform precision measurements [9–11]. A precise control of the electronic, vibrational, rotational and hyperfine states of polar molecules is of great importance to these applications [12, 13]. Stimulated Raman adiabatic passage (STIRAP) allows for a coherent population transfer between two molecular internal quantum states [14, 15], and has been employed to create and detect the ultracold alkali-metal-diatomic molecules in the rovibrational ground state [1, 4, 16–22]. The principle of STIRAP can be understood using a three-level model, which involves the Feshbach state, the intermediate electronic excited state, and the molecular rovibrational ground state [14, 16]. However, in realistic molecules, both the electronic excited state and the rovibrational ground state have many hyperfine levels [23, S5, S1]. These complex level structures raise several open questions on how STIRAP works in a realistic molecule system.

The first open question is about the intermediate electronic excited state. In a molecule, each rovibrational level of the electronic excited state contains many hyperfine levels. Therefore, in practice, a well-resolved hyperfine level of the excited state is selected as the intermediate state by setting the single-photon detuning

to be zero [16–21]. This hyperfine excited state should be dominantly coupled to one of the hyperfine levels of the ground state, and thus a resonantly coupled three-level system is selected. It is usually assumed that if the energy difference between the selected and the adjacent hyperfine level of the excited state is much larger than the natural linewidth of the excited states and the Rabi frequencies of the STIRAP lasers, then only the resonant STIRAP plays a dominant role, and the other excited states can be safely neglected.

STIRAP can also proceed via other hyperfine levels of the excited state with a single-photon detuning [14, 15, 22, 26]. In previous works, detuned STIRAPs are usually neglected, once a well-resolved hyperfine excited state has been selected for the resonant STIRAP. However, detuned STIRAP always exists in the realistic molecule systems and may contribute the unexpected transfer channels. Since STIRAP is a coherent process, the different channels due to the resonant and detuned STIRAP may interfere with each other and cause unexpected interference phenomenon. Despite that STIRAPs in multi-level systems have been intensively studied in previous works [14, 15] and the various scenarios, such as the resonant and off-resonant multistate chains [27–29], the multiple intermediate states [26], and the multiple ground states [30, 31], have been investigated, the interference between resonant STIRAP and detuned STIRAP has not been observed before.

The second open question is about the hyperfine levels

[*] These authors contributed equally to this work.

of the ground state. Since in principle more than one hyperfine level of the molecular ground state can be populated in the STIRAP transfer, a natural question is how to quantitatively characterize the purity of the hyperfine levels of the ground state. It seems that this question cannot be answered by just observing the Feshbach molecules, since the ground-state molecule cannot be directly detected. Another relevant question is, if the STIRAP does not prepare the molecule in a single hyperfine level of the ground state, whether the molecule is in a coherent superposition or in an incoherent mixture of different hyperfine states? To answer this question is particularly important to the fermionic molecules, as the fermionic molecules in a superposition state are still identical fermions, and thus s -wave collisions among them are suppressed due to the Pauli principle [32, 33]. Incoherent mixtures, in contrast, suffer from s -wave collisions. Therefore whether the created state is a coherent superposition state or an incoherent mixture is important to interpret the lifetime of the ground state molecules [19].

In this Letter, we report on the first observation of the interference between resonant and detuned STIRAP in the adiabatic creation of $^{23}\text{Na}^{40}\text{K}$ ground-state molecules. The interference manifests itself as the oscillation of the number of Feshbach molecules after a round-trip STIRAP versus the hold time between the forward and the reverse STIRAP. Surprisingly, the oscillation has a high visibility of about 90% even if the single-photon detuning of the detuned STIRAP is about one order of magnitude larger than the linewidth of the excited state and the Rabi frequencies of the STIRAP lasers. At the same time, the STIRAP spectrum shows two peaks, and the spectrum changes with the hold time. The interference phenomenon indicates that if more than one hyperfine level of the ground state is populated, the STIRAP creates a superposition state, but not an incoherent mixture. Moreover, the interference provides a tool to quantitatively characterize the purity of the hyperfine levels of the ground-state molecule.

Our experiment starts with $^{23}\text{Na}^{40}\text{K}$ Feshbach molecules which are associated from an ultracold atomic mixture in a crossed-beam optical dipole trap at a magnetic field of 89.77(1) G, which is close to the atomic s -wave Feshbach resonance between $|f, m_f\rangle_{\text{Na}} = |1, 1\rangle$ and $|f, m_f\rangle_{\text{K}} = |9/2, -7/2\rangle$ at 90.33 G [34]. The binding energy of the Feshbach molecule is about 122 kHz, and about 2.3×10^4 Feshbach molecules can be formed. To transfer the molecules from the Feshbach state $|F\rangle$ to the rovibrational ground state, we employ a mixture of the electronic excited states $B^1\Pi |v = 12, J = 1\rangle$ and $c^3\Sigma |v = 35, J = 1\rangle$. The hyperfine structure of the electronic excited state has been extensively investigated in Refs. [S6, S5].

We choose the hyperfine level $|E_r\rangle$ of the electronic excited state as the intermediate state, which may be

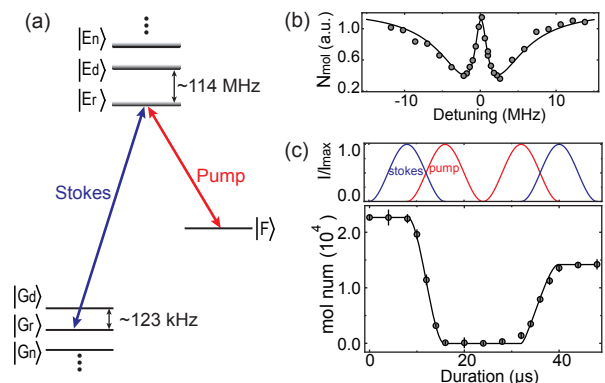


FIG. 1: (a) Illustration of stimulated Raman adiabatic passage (STIRAP) in the adiabatic creation of the $^{23}\text{Na}^{40}\text{K}$ molecule. The $|E_r\rangle$, $|E_d\rangle$ and $|E_n\rangle$ states are the hyperfine levels of the electronic excited state, and the $|G_r\rangle$, $|G_d\rangle$ and $|G_n\rangle$ states are the hyperfine levels of the rovibrational ground state. The $|E_r\rangle$ state is well-separated from the other hyperfine excited states. The pump light resonantly couples the Feshbach state $|F\rangle$ and the intermediate electronic state $|E_r\rangle$, and the Stokes light resonantly couples the ground state $|G_r\rangle$ and $|E_r\rangle$. (b) Two-photon dark-state spectroscopy. (c) The pulse sequence of the round-trip STIRAP. The number of Feshbach molecules during the STIRAP process is measured by truncating the laser pulses. Error bars represent ± 1 s.d.

approximately described by the quantum numbers $F_1 \approx 1/2$, $m_{F_1} \approx -1/2$, $m_{I_K} \approx -2$ and a total angular momentum projection $m_F = -5/2$. As shown in Fig. 1(a), the energy difference between this hyperfine state and the nearest neighbouring hyperfine excited state is 114(10) MHz, which is much larger than the linewidth 10(1) MHz of the excited state, and thus the $|E_r\rangle$ hyperfine state is well-separated from other hyperfine excited states. The pump laser coupling the $|F\rangle$ state to the $|E_r\rangle$ state, and the Stokes laser coupling $|E_r\rangle$ and the ground state are both π -polarized. Because the $|E_r\rangle$ state has $m_{I_K} \approx -2$ and $m_F = -5/2$, the hyperfine level of the ground state that is dominantly populated by the Stokes light is given by $|G_r\rangle = |v, N, m_{I_{\text{Na}}}, m_{I_K}\rangle = |0, 0, -1/2, -2\rangle$, where v and N are the vibrational and rotational quantum numbers. In this case, we expect the $|E_r\rangle$, $|G_r\rangle$ and $|F\rangle$ states to form an almost ideal three-level system.

In the experiment, the pump laser (805 nm) and the Stokes laser laser (567 nm) are locked to an ultralow expansion (ULE) cavity. The peak Rabi frequency of the pump light is $\Omega_P = 2\pi \times 4.6(3)$ MHz, and the peak Rabi frequency of the Stokes light is $\Omega_S = 2\pi \times 9.3(4)$ MHz. They are determined from the two-photon dark-state spectroscopy as shown in Fig. 1(b). We first perform a round-trip STIRAP using the pulse sequence in Fig. 1(c). The number of the remaining Feshbach molecules during the STIRAP process is measured by truncating the pump and the Stokes laser pulses and detecting the molecules in

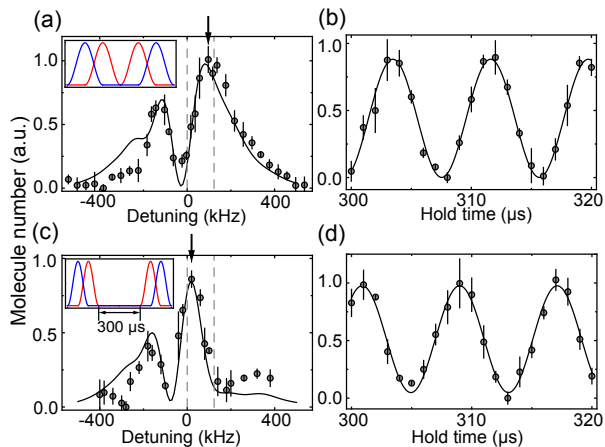


FIG. 2: (a) The STIRAP spectrum is measured as a function of the frequency of the pump laser. The solid line is a theoretical fit to the shape of the data (see text). The two vertical dashed lines represent two-photon resonances between the Feshbach state $|F\rangle$ and the hyperfine levels $|G_r\rangle$ and $|G_d\rangle$ of the ground state, respectively. The pulse sequence is shown in the inset. (b) The number of Feshbach molecules after a round-trip STIRAP as a function of hold time between the forward and reverse STIRAP oscillates with a visibility of 90% and a frequency of about 123 kHz. The pump laser frequency used for this measurement is marked by the arrow in (a). (c) The STIRAP spectrum is measured for a hold time of 300 μ s. The pulse sequence is shown in the inset. (d) The number of Feshbach molecules after a round-trip STIRAP as a function of hold time. The pump laser frequency used for this measurement is marked by the arrow in (c). Error bars represent ± 1 s.d.

the $|F\rangle$ state. The results show that, starting from about 2.3×10^4 Feshbach molecules, after a round-trip STIRAP about 1.4×10^4 Feshbach molecules are recovered. This corresponds to a one-way (round-trip) transfer efficiency of about 78% (61%), which indicates that about 1.8×10^4 ground-state molecules are created.

So far, the experimental results are consistent with our understanding based on a simple three-level model. We then measure the STIRAP spectrum by scanning the frequency of the pump laser. As shown in Fig. 2(a), we observe two well-separated peaks in the spectrum, with a frequency difference of about 240 kHz. The observation of two peaks is unexpected, since the Stokes laser dominantly couples the $|E_r\rangle$ state with the $|G_r\rangle$ state, and a numerical calculation shows that the coupling strength between the $|E_r\rangle$ and $|G_r\rangle$ states is about one order of magnitude larger than to other hyperfine levels of the ground state.

We set the frequency of the pump laser to the higher peak and measure the lifetime of the ground-state molecule by varying the hold time between the forward and reverse STIRAP. We observe that the number of the Feshbach molecules after a round-trip STIRAP oscillates as a function of the hold time, with a high visibility

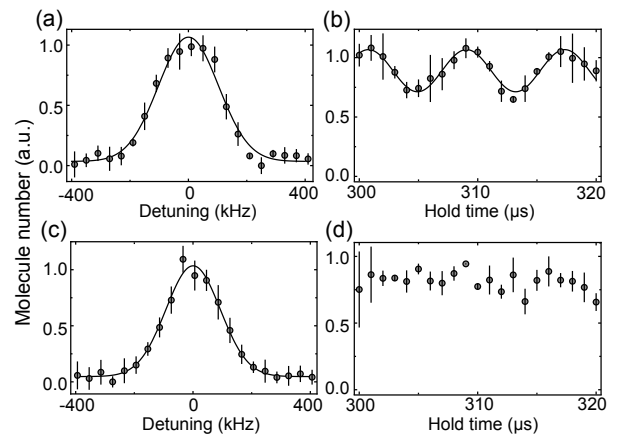


FIG. 3: Increase of the purity by reducing the Rabi frequencies of the STIRAP lasers. (a) The STIRAP spectrum and (b) the measured oscillation with $\Omega_P, \Omega_S \approx 2\pi \times 4.6$ MHz. The estimated purity of the hyperfine ground state is about 90%. (c) The STIRAP spectrum and (d) the measured oscillation with $\Omega_P, \Omega_S \approx 2\pi \times 3.3$ MHz. There is no obvious oscillation in (d). The estimated purity of the hyperfine level of the ground state is about 99%. Error bars represent ± 1 s.d.

of about 90% and a frequency of about 123 kHz, as is shown in Fig. 2(b). This indicates the efficiency of the reverse STIRAP oscillates with the hold time. Note that an oscillation of the Feshbach molecule number after a round-trip transfer was also reported in Ref. [21]. In that work, the oscillation frequency is consistent with the axial trapping frequency, and the oscillation is attributed to the axial sloshing. However, in our experiment, the oscillation frequency is about three orders of magnitude larger than the trap frequencies.

To understand these phenomena, we measure the STIRAP spectrum using a different pulse sequence. As shown in Fig. 2(c), the shape of the spectrum changes and the higher peak is shifted by about 60 kHz. By setting the frequency of the pump laser to this higher peak, we measure the number of Feshbach molecules as a function of the hold time, which still oscillates with the same frequency but with a different phase (see Fig. 2(d)).

These results strongly suggest that what we observe is a quantum interference phenomenon. The oscillation frequency of about 123 kHz is very close to the energy difference between the $|G_r\rangle$ state and the adjacent hyperfine level of the ground state $|G_d\rangle = |0, 0, -3/2, -1\rangle$ at $B = 89.77$ G [19, S1]. Therefore, these phenomena may be due to interference involving these two hyperfine levels. However, the coupling strength between the $|E_r\rangle$ and $|G_d\rangle$ states is negligible, and thus the resonant STIRAP will not populate the $|G_d\rangle$ state.

After carefully studying the molecule structure and the STIRAP process, we find these phenomena can

be explained by taking the detuned STIRAP between the $|F\rangle$ and $|G_d\rangle$ states via the neighbouring hyperfine excited state $|E_d\rangle$ into account, described by the quantum numbers $F_1 \approx 3/2, m_{F_1} \approx -3/2, m_{I_K} \approx -1$. Because the $|E_d\rangle$ state has $m_{I_K} \approx -1$, the detuned STIRAP dominantly transfers the molecule to the $|G_d\rangle$ state. Therefore, the interference between the resonant and detuned STIRAP induces the coherence between $|G_r\rangle$ and $|G_d\rangle$. The $|E_d\rangle$ level is higher than the $|E_r\rangle$ level by 114(10) MHz, and it is lower than the next higher excited state $|E_n\rangle$ by about 80 MHz. The single-photon detuning of the detuned STIRAP via the $|E_d\rangle$ is one order of magnitude larger than the Rabi frequencies of the lasers and the linewidth of the excited state. For such a large detuning, it is surprising that the detuned STIRAP cannot be neglected if compared with the resonant STIRAP.

The observed oscillation may be understood as follows. Starting from the $|F\rangle$ state, the resonant STIRAP transfers the molecules from the $|F\rangle$ to the $|G_r\rangle$ state, while the detuned STIRAP transfers them from the $|F\rangle$ to the $|G_d\rangle$ state. These two processes interfere with each other, and consequently the forward STIRAP creates a superposition state between $|G_r\rangle$ and $|G_d\rangle$, which may be described by $|G\rangle_{in} = \cos\theta_1|G_r\rangle + e^{i\phi_1}\sin\theta_1|G_d\rangle$, with θ_1 and ϕ_1 being unknown parameters. After the forward STIRAP, the superposition state freely evolves according to $|G(t)\rangle_{in} = \cos\theta_1|G_r\rangle + e^{i(2\pi\nu_{rd}t+\phi_1)}\sin\theta_1|G_d\rangle$, where ν_{rd} is the frequency difference between the $|G_r\rangle$ and the $|G_d\rangle$ state. Assuming that the reverse STIRAP converts the $|G\rangle_{out} = \cos\theta_2|G_r\rangle + e^{i\phi_2}\sin\theta_2|G_d\rangle$ state back to the $|F\rangle$ state, we expect that the conversion efficiency for a hold time of t is proportional to $|\langle G_{in}(t)|G_{out}\rangle|^2 = \cos^2\theta_1\cos^2\theta_2 + \sin^2\theta_1\sin^2\theta_2 + \sin 2\theta_1\sin 2\theta_2\cos(2\pi\nu_{rd}t + \phi_1 - \phi_2)/2$, which oscillates with a frequency of ν_{rd} .

To quantitatively explain the experimental results, we numerically calculate the STIRAP spectrum [36]. In our calculation, we include three neighbouring hyperfine excited states $|E_i\rangle$ with $i = r, d, n$ and three neighbouring hyperfine ground states $|G_i\rangle$ with $i = r, d, n$, which can be coupled by the Stokes and the pump light. The relative coupling strengths between the different states are calculated by using the method introduced in Ref. [22, 36, S5]. The shape of the theoretical STIRAP spectrum is fitted to the experimental data, as shown in Fig. 2(a) and 2(c). The two peak structures of the STIRAP spectrum are reproduced by the theoretical calculations. The valley between the two peaks is caused by destructive interference, and the peaks are shifted from two-photon resonances due to the interference. The numerical calculations show that the forward STIRAP mainly creates a superposition between the $|G_r\rangle$ and $|G_d\rangle$ states, and that the efficiency of the round-trip STIRAP oscillates with a frequency equal to ν_{rd} .

The observed interference demonstrates that in the STIRAP transfer, if more than one hyperfine level

of the ground state can be populated, the forward STIRAP creates a superposition of the different hyperfine states. It is still a fully polarized state, but not an incoherent mixture. For the fermionic molecules, the s -wave collision between the ground-state molecules in a superposition state is still suppressed due to the Pauli principle [32, 33].

The observed oscillation provides a method to quantitatively characterize the purity of the hyperfine levels of the created state. Assuming $\theta_1 = \theta_2 = \theta$, the visibility of the oscillation may be expressed as $vis = (1 - \cos 4\theta)/(3 + \cos 4\theta)$. The visibility in our experiment is about 0.90, and a simple calculation yields $|G\rangle_{in} = \sqrt{0.61}|G_r\rangle + e^{i\phi_1}\sqrt{0.39}|G_d\rangle$. Therefore we determine the purity of the ground-state molecule in the $|G_r\rangle$ state to be about 0.61.

The purity can be increased by reducing the Rabi frequencies of the lasers. The STIRAP spectrum and the efficiency versus the hold time for different Rabi frequencies are plotted in Fig. 3. By reducing the Rabi frequencies to $\Omega_P, \Omega_S \approx 2\pi \times 3.3$ MHz, no obvious oscillation can be observed, as shown in Fig. 3(d). If we still fit the data points with an oscillation function, we obtain a visibility of 0.03, and thus the purity in $|G_r\rangle$ is 0.99, which is very high.

The created superposition state created is between the $|G_r\rangle$ and $|G_d\rangle$ states. These two states have only nuclear spins, and their frequency difference is insensitive to the magnetic field. We measure the oscillation for a long hold time. As shown in Fig. 4, the oscillation can be clearly observed after 150 ms which corresponds to more than 10^4 oscillations. By fitting the data points with a single oscillation function, we obtain the frequency of 123.080(1) kHz. From this frequency, we determine the scalar coefficient $c_4 = 416(35)$ Hz in the molecule Hamiltonian, which is consistent with the result in Ref. [37]. The superposition between different hyperfine ground states may be employed to implement a STIRAP interferometer. The superposition state created in our work is due to the interference between resonant and detuned STIRAP. The superposition state may also be created by employing polarizations of lasers. For example, a superposition state may be easily created in STIRAP by employing the $(\sigma^+ + \sigma^-)/\sqrt{2}$ polarized pump light to couple the Feshbach state to two hyperfine excited states, and by employing the π polarized Stokes light to couple each hyperfine excited state to one hyperfine ground state. Besides, a similar interferometer could be created by stopping STIRAP half-way [38, 39].

In summary, we have observed interference between resonant and detuned STIRAP in the adiabatic creation of $^{23}\text{Na}^{40}\text{K}$ ground-state molecules. Such an interference phenomenon adds an unexpected new basic aspect to STIRAP, which has been overlooked in the past. The interference clearly demonstrates that if more than one hyperfine state is populated, the state created

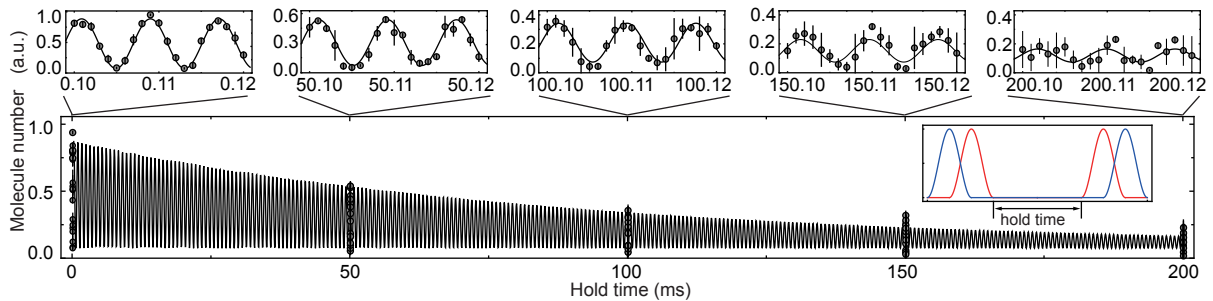


FIG. 4: The coherence between the $|G_r\rangle$ and the $|G_d\rangle$ state is measured for a long hold time. We fit the data points with a single oscillation function, which gives a frequency of 123.080(1) kHz. The oscillation can be clearly observed for 150 ms, which corresponds to more than 10^4 oscillations. The pulse sequence is shown in the inset. Error bars represent ± 1 s.d.

by STIRAP is a superposition state, and thus the s -wave collisions between the fermionic molecules are still suppressed due to the Pauli principle. The superposition state can be changed to an incoherent mixture by introducing decoherence mechanisms. The mixture might be useful in evaporative cooling, as demonstrated the ^6Li atomic gases [32, 40]. The observed oscillation provides a method to quantitatively measure the purity of the ground-state molecules. The STIRAP interferometer may also be employed to detect collisions between molecules.

This work was supported by the National Key R&D Program of China (under Grant No. 2018YFA0306502), the National Natural Science Foundation of China (under Grant No. 11521063), the Chinese Academy of Sciences, the Anhui Initiative in Quantum Information Technologies, and Shanghai Sailing Program (under Grant No. 17YF1420900).

[1] S. Ospelkaus, K.-K. Ni, D. Wang, M. H. G. de Miranda, B. Neyenhuis, G. Quémener, P. S. Julienne, J. L. Bohn, D. S. Jin, and J. Ye, *Science* **327**, 853 (2010).
 [2] S. Knoop, F. Ferlaino, M. Berninger, M. Mark, H.-C. Nägerl, R. Grimm, J. P. D’Incao, and B. D. Esry, *Phys. Rev. Lett.* **104**, 053201 (2010).
 [3] J. Rui, H. Yang, L. Liu, D.-C. Zhang, Y.-X. Liu, J. Nan, Y.-A. Chen, B. Zhao, and J.-W. Pan, *Nature Physics* **13**, 699 (2017).
 [4] H. Yang, D.-C. Zhang, L. Liu, Y.-X. Liu, J. Nan, B. Zhao, and J.-W. Pan, *Science* **363**, 261 (2019).
 [5] A. Micheli, G. K. Brennen, and P. Zoller, *Nature Physics* **2**, 341 (2006).
 [6] M. A. Baranov, M. Dalmonte, G. Pupillo, and P. Zoller, *Chem. Rev.* **112**, 5012 (2012).
 [7] D. DeMille, *Phys. Rev. Lett.* **88**, 067901 (2002).
 [8] P. Rabl, D. DeMille, J. M. Doyle, M. D. Lukin, R. J. Schoelkopf, and P. Zoller, *Phys. Rev. Lett.* **97**, 033003 (2006).
 [9] D. DeMille, S. Sainis, J. Sage, T. Bergeman, S. Kotochigova, and E. Tiesinga, *Phys. Rev. Lett.* **100**, 043202 (2008).

[10] T. Zelevinsky, S. Kotochigova, and J. Ye, *Phys. Rev. Lett.* **100**, 043201 (2008).
 [11] J. Baron, W. C. Campbell, D. DeMille, J. M. Doyle, G. Gabrielse, Y. V. Gurevich, P. W. Hess, N. R. Hutzler, E. Kirilov, I. Kozyryev, et al., *Science* **343**, 269 (2014).
 [12] L. D. Carr, D. DeMille, R. V. Krems, and J. Ye, *New J. Phys.* **11**, 1367 (2009).
 [13] G. Quémener and P. S. Julienne, *Chem. Rev.* **112**, 4949 (2012).
 [14] K. Bergmann, H. Theuer, and B. W. Shore, *Rev. Mod. Phys.* **70**, 1003 (1998).
 [15] N. V. Vitanov, A. A. Rangelov, B. W. Shore, and K. Bergmann, *Rev. Mod. Phys.* **89**, 015006 (2017).
 [16] K.-K. Ni, S. Ospelkaus, M. H. G. de Miranda, A. Pe’er, B. N. J. J. Zirbel, S. Kotochigova, P. S. Julienne, D. S. Jin, and J. Ye, *Science* **322**, 231 (2008).
 [17] P. K. Molony, P. D. Gregory, Z. Ji, B. Lu, M. P. Köppinger, C. R. Le Sueur, C. L. Blackley, J. M. Hutson, and S. L. Cornish, *Phys. Rev. Lett.* **113**, 255301 (2014).
 [18] T. Takekoshi, L. Reichsöllner, A. Schindewolf, J. M. Hutson, C. R. Le Sueur, O. Dulieu, F. Ferlaino, R. Grimm, and H.-C. Nägerl, *Phys. Rev. Lett.* **113**, 205301 (2014).
 [19] J. W. Park, S. A. Will, and M. W. Zwierlein, *Phys. Rev. Lett.* **114**, 205302 (2015).
 [20] M. Guo, B. Zhu, B. Lu, X. Ye, F. Wang, R. Vexiau, N. Bouloufa-Maafa, G. Quémener, O. Dulieu, and D. Wang, *Phys. Rev. Lett.* **116**, 205303 (2016).
 [21] T. M. Rvachov, H. Son, A. T. Sommer, S. Ebadi, J. J. Park, M. W. Zwierlein, W. Ketterle, and A. O. Jamison, *Phys. Rev. Lett.* **119**, 143001 (2017).
 [22] F. Seeßelberg, N. Buchheim, Z.-K. Lu, T. Schneider, X.-Y. Luo, E. Tiemann, I. Bloch, and C. Gohle, *Phys. Rev. A* **97**, 013405 (2018).
 [23] S. Ospelkaus, K.-K. Ni, G. Quémener, B. Neyenhuis, D. Wang, M. H. G. de Miranda, J. L. Bohn, J. Ye, and D. S. Jin, *Phys. Rev. Lett.* **104**, 030402 (2010).
 [S5] J. W. Park, S. A. Will, and M. W. Zwierlein, *New J. Phys.* **17**, 075016 (2015).
 [S1] J. Aldegunde and J. M. Hutson, *Phys. Rev. A* **96**, 042506 (2017).
 [26] N. V. Vitanov and S. Stenholm, *Phys. Rev. A* **60**, 3820 (1999).
 [27] B. W. Shore, K. Bergmann, J. Oreg, and S. Rosenwaks, *Phys. Rev. A* **44**, 7442 (1991).
 [28] P. Pillet, C. Valentin, R. I. Yuan, and J. Yu, *Phys. Rev. A* **48**, 845 (1993).

- [29] N. V. Vitanov, B. W. Shore, and K. Bergmann, Eur. Phys. J. D **4**, 15 (1998).
- [30] J. Martin, B.W. Shore, and K. Bergmann, Phys. Rev. A **52**, 583 (1995).
- [31] J. Martin, B.W. Shore, and K. Bergmann, Phys. Rev. A **54**, 1556 (1996).
- [32] S. Gupta, Z. Hadzibabic, M. W. Zwierlein, C. A. Stan, K. Dieckmann, C. H. Schunck, E. G. M. van Kempen, B. J. Verhaar, and W. Ketterle, Science **300**, 1723 (2003).
- [33] M. W. Zwierlein, Z. Hadzibabic, S. Gupta, and W. Ketterle, Phys. Rev. Lett. **91**, 250404 (2003).
- [34] J. W. Park, C.-H. Wu, I. Santiago, T. G. Tiecke, S. Will, P. Ahmadi, and M. W. Zwierlein, Phys. Rev. A **85**, 051602 (2012).
- [S6] K. Ishikawa, T. Kumauchi, M. Baba, , and H. Katô, J. Chem. Phys. **96**, 6423 (1992).
- [36] See details in supplementary materials.
- [37] J. W. Park, Z. Z. Yan, H. Loh, S. A. Will, and M. W. Zwierlein, Science **357**, 372 (2017).
- [38] K. Winkler, G. Thalhammer, M. Theis, H. Ritsch, R. Grimm, and J. Hecker Denschlag, Phys. Rev. Lett. **95**, 063202 (2005).
- [39] M. Semczuk, W. Gunton, W. Bowden, and K. W.

- Madison, Phys. Rev. Lett. **113**, 055302 (2014).
- [40] W. Ketterle, and M. Zwierlein, arXiv.org/0801.2500 (2008).

SUPPLEMENTARY MATERIALS

A. STIRAP

To quantitatively understand the experimental results, we use a seven-level model to numerically simulate the STIRAP process. In the supplementary materials, we denote the three hyperfine levels of the excited states $|E_r\rangle$, $|E_d\rangle$ and $|E_n\rangle$ by $|e_1\rangle$, $|e_2\rangle$ and $|e_3\rangle$, respectively, and we denote the three hyperfine levels of the ground state $|G_r\rangle$, $|G_d\rangle$ and $|G_n\rangle$ by $|g_1\rangle$, $|g_2\rangle$ and $|g_3\rangle$ respectively. The Feshbach state $|F\rangle$ is denoted by $|f\rangle$. The pump light couples $|e_{1,2,3}\rangle$ to $|f\rangle$, and the Stokes light couples $|e_{1,2,3}\rangle$ to $|g_{1,2,3}\rangle$. In the rotating frame, the Hamiltonian governing the STIRAP process is given by

$$H(t) = \begin{pmatrix} \delta_f & \frac{\Omega_{e_1 f}(t)}{2} & \frac{\Omega_{e_2 f}(t)}{2} & \frac{\Omega_{e_3 f}(t)}{2} & 0 & 0 & 0 \\ \frac{\Omega_{e_1 f}(t)}{2} & \Delta_{e_1} - i\frac{\Gamma}{2} & 0 & 0 & \frac{\Omega_{e_1 g_1}(t)}{2} & \frac{\Omega_{e_1 g_2}(t)}{2} & \frac{\Omega_{e_1 g_3}(t)}{2} \\ \frac{\Omega_{e_2 f}(t)}{2} & 0 & \Delta_{e_2} - i\frac{\Gamma}{2} & 0 & \frac{\Omega_{e_2 g_1}(t)}{2} & \frac{\Omega_{e_2 g_2}(t)}{2} & \frac{\Omega_{e_2 g_3}(t)}{2} \\ \frac{\Omega_{e_3 f}(t)}{2} & 0 & 0 & \Delta_{e_3} - i\frac{\Gamma}{2} & \frac{\Omega_{e_3 g_1}(t)}{2} & \frac{\Omega_{e_3 g_2}(t)}{2} & \frac{\Omega_{e_3 g_3}(t)}{2} \\ 0 & \frac{\Omega_{e_1 g_1}(t)}{2} & \frac{\Omega_{e_2 g_1}(t)}{2} & \frac{\Omega_{e_3 g_1}(t)}{2} & \delta_{g_1} & 0 & 0 \\ 0 & \frac{\Omega_{e_1 g_2}(t)}{2} & \frac{\Omega_{e_2 g_2}(t)}{2} & \frac{\Omega_{e_3 g_2}(t)}{2} & 0 & \delta_{g_2} & 0 \\ 0 & \frac{\Omega_{e_1 g_3}(t)}{2} & \frac{\Omega_{e_2 g_3}(t)}{2} & \frac{\Omega_{e_3 g_3}(t)}{2} & 0 & 0 & \delta_{g_3} \end{pmatrix} \quad (S1)$$

In the case that the pump light resonantly couples $|e_1\rangle$ to $|f\rangle$, and the Stokes light resonantly couples $|e_1\rangle$ to $|g_1\rangle$, we have $\Delta_{e_1} = \delta_{g_1} = \delta_f = 0$. The linewidth of the excited state $\Gamma = 2\pi \times 10$ MHz, the detuning of the other two excited states $\Delta_{e_2} = 11.4\Gamma$, $\Delta_{e_3} = 19.6\Gamma$, and the peak Rabi frequencies $\Omega_{e_1 f} = \Omega_P = 0.46\Gamma$, $\Omega_{e_1 g_1} = \Omega_S = 0.93\Gamma$ can be determined in the experiment. The other parameters are determined by theoretical calculations. The detuning of the other two hyperfine levels of the ground state are $\delta_{g_2} = 0.012308\Gamma$ and $\delta_{g_3} = -0.012224\Gamma$. The values of the relative coupling strengths are listed in Table S1. The details of the calculations are given in Sec. B, C, and D of the supplementary materials.

In our experiment, the time dependent intensity of the pump and Stokes light is approximately given by

$$\frac{I(t)}{I_{max}} = \frac{1 - \cos(\pi(t - t_i)/t_d)}{2} \quad (S2)$$

for $t_i < t < t_i + 2t_d$ with $t_d = 8 \mu\text{s}$, which is obtained by controlling the rf power driving the acoustic-optical modulator.

$\Omega_{e_2 f}/\Omega_{e_1 f}$	0.712
$\Omega_{e_3 f}/\Omega_{e_1 f}$	0.416
$\Omega_{e_1 g_2}/\Omega_{e_1 g_1}$	-0.144
$\Omega_{e_1 g_3}/\Omega_{e_1 g_1}$	-0.009
$\Omega_{e_2 g_1}/\Omega_{e_1 g_1}$	0.023
$\Omega_{e_2 g_2}/\Omega_{e_1 g_1}$	-1.16
$\Omega_{e_2 g_3}/\Omega_{e_1 g_1}$	0.0455
$\Omega_{e_3 g_1}/\Omega_{e_1 g_1}$	0.514
$\Omega_{e_3 g_2}/\Omega_{e_1 g_1}$	0.199
$\Omega_{e_3 g_3}/\Omega_{e_1 g_1}$	0.297

TABLE S1: The calculated relative coupling strengths.

Given these parameters, we can numerically simulate the STIRAP process by solving the time dependent Schrödinger equation

$$i\dot{|\psi(t)\rangle} = H(t)|\psi(t)\rangle, \quad (S3)$$

where the wave function is expressed as

$$|\psi(t)\rangle = c_f(t)|f\rangle + \sum_i c_{g_i}(t)|g_i\rangle + \sum_j c_{e_j}(t)|e_j\rangle \quad (S4)$$

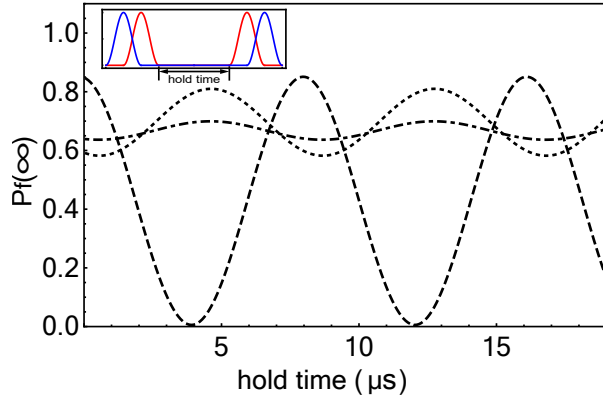


FIG. S1: The probability in the Feshbach state after a round-trip STIRAP $P_f(\infty) = |c_f(\infty)|^2$ as a function of the hold time are calculated using the theoretical model. The parameters used in the calculations are $\Omega_S = 0.93\Gamma$, $\Omega_P = 0.46\Gamma$ (dashed line), $\Omega_S = \Omega_P = 0.46\Gamma$ (dotted line), and $\Omega_S = \Omega_P = 0.33\Gamma$ (dotdashed line). The inset is the pulse sequence.

with the initial condition $c_f(0) = 1$ and $c_{g_{1,2,3}}(0) = c_{e_{1,2,3}}(0) = 0$.

The number of Feshbach molecules after a round-trip STIRAP is proportional to the probability in the Feshbach state $P_f(\infty) = |c_f(\infty)|^2$. In Fig. S1, We plot the calculated $P_f(\infty)$ as a function of hold time. The dashed line is the theoretical curve for the Rabi frequencies $\Omega_S = 0.93\Gamma$ and $\Omega_P = 0.46\Gamma$. The oscillation frequency is given by 123.08 kHz, which is equal to the frequency difference between $|g_1\rangle$ and $|g_2\rangle$. The calculated STIRAP efficiency is higher than the experimental result, which may be due to the remaining phase noises of the pump and Stokes lasers.

The STIRAP spectrum is given by plotting $P_f(\infty)$ as a function of δ_f . The spectrum show two peak structures and is also a period function of the hold time, which is consistent with the experimental results. The shape of the calculated spectrum is fitted to the experimental data, as shown in the Fig. 2(a) and 2(c) of the main text.

Given the theoretical model, we find that the effect of interference can be suppressed by reducing the Rabi frequencies of the pump and Stokes lasers. As shown in Fig. S1, by reducing the Rabi frequencies to $\Omega_S = \Omega_P = 0.33\Gamma$, the interference is largely suppressed. In our experiment, when reducing the Rabi frequencies to $\Omega_S, \Omega_P \approx 0.33\Gamma$, no obvious oscillations can be observed, as shown in Fig. 3 of the main text.

In the following sections, we will give the details of the calculations to determine the energy differences δ_{g_2} and δ_{g_3} and the relative coupling strengths listed in Table S1.

B. GROUND STATE

The rovibrational ground state has good quantum numbers $N = S = J = M_J = 0$. The quantum state of the hyperfine level of the ground state can be expressed as $|NSJM_J m_{i_{Na}} m_{i_{K}}\rangle$, where the projections of nuclear spins $m_{i_{Na}}$ and $m_{i_{K}}$ are also approximately good quantum numbers at the large magnetic fields. The energy difference δ_{g_2} and δ_{g_3} of different hyperfine levels are calculated using the Hamiltonian [S1]

$$H_g = g_{i_{Na}} \mu_B i_{z_{Na}} B_z + g_{i_{K}} \mu_B i_{z_{K}} B_z - c_4 \mathbf{i}_{Na} \cdot \mathbf{i}_{K} \quad (S5)$$

where $g_{i_{Na}} = -0.00080461$ and $g_{i_{K}} = 0.00017649$ are the nuclear g-factors and B_z is the bias magnetic field. We have used the measured value $c_4 = 416$ Hz in the calculation.

C. FESHBACH STATE

To calculate the relative coupling strengths between the different hyperfine levels of the excited states and the Feshbach state, we first calculate the wave function of the Feshbach state using the coupled-channel method. The Hamiltonian describing the s -wave bound state is

$$H = T + \sum_{S=0,1} V_S(r) P_S + H_{hf} + H_z. \quad (S6)$$

The first term is the kinetic energy $T = -\frac{\hbar^2}{2\mu} \frac{d^2}{dr^2}$ with μ the reduced mass. The second term describes the spin-exchanging interaction, where $P_0 = 1/4 - \mathbf{s}_{Na} \cdot \mathbf{s}_{K}$ and $P_1 = 3/4 + \mathbf{s}_{Na} \cdot \mathbf{s}_{K}$ are the singlet and triplet projection operator respectively with \mathbf{s} the electron spin. $V_0(r)$ and $V_1(r)$ denotes the Born-Oppenheimer singlet potential $X^1\Sigma$ and triplet potential $a^3\Sigma$. The Born-Oppenheimer potentials can be expressed as power expansions of r , whose exact form can be found in Ref. [S2, S3]. H_{hf} is the hyperfine interaction term, described by

$$H_{hf} = a_{Na} \mathbf{s}_{Na} \cdot \mathbf{i}_{Na} + a_K \mathbf{s}_K \cdot \mathbf{i}_K, \quad (S7)$$

where $a_{Na,K}$ is the hyperfine constant and \mathbf{i} is the nuclear spin. The last term is the Zeeman term

$$H_z = [(g_s s_{z_{Na}} - g_{i_{Na}} i_{z_{Na}}) + (g_s s_{z_{K}} - g_{i_{K}} i_{z_{K}})] \mu_B B_z, \quad (S8)$$

with g_s the electron g-factor, g_i the nuclear g-factor and B_z the bias magnetic field.

The internal state may be expressed in terms of the spin basis $|\sigma\rangle = |S, M_S, m_{i_{Na}}, m_{i_{K}}\rangle$. The Hamiltonian couples all the internal states with the same $M_F = M_S + m_{i_{Na}} + m_{i_{K}}$. For a given M_F and B_z , we first diagonalize the $H_{hf} + H_z$ to obtain the internal eigenstate $|\chi_i\rangle$ and the threshold energy E_i^{th} of each channel. Expanding the wave function in terms of the new bases $|\psi_f\rangle =$

$\sum_i \psi_i(r)|\chi_i\rangle$, we obtain the coupled channel Schrödinger equation

$$\sum_j [T\delta_{ij} + \sum_{S=0,1} V_S(r)\langle\chi_i|P_S|\chi_j\rangle]\psi_j(r) = (E - E_i^{th})\psi_i(r) \quad (\text{S9})$$

The binding energy and the wave function of the Feshbach state are calculated by means of the renormalized Numerov method [S4].

The closed-channel component of the Feshbach state is dominated by the highest bound state in the triplet potential. This bound state has good quantum numbers $N = 0, S = 1$ and $J = 1$. The closed-channel component of the wave function of the Feshbach state can be expressed as

$$|\psi_f\rangle \propto \sum_{M_J m_{i_{\text{Na}}} m_{i_{\text{K}}}} c_{NSJM_J m_{i_{\text{Na}}} m_{i_{\text{K}}}}^f |NSJ, M_J m_{i_{\text{Na}}} m_{i_{\text{K}}}\rangle. \quad (\text{S10})$$

For the Feshbach state between ^{23}Na $|1, 1\rangle$ and ^{40}K $|9/2, -7/2\rangle$ at 89.77 G with a binding energy of 122 kHz, the calculated coefficients in the uncoupled basis are

M_J	$m_{i_{\text{Na}}}$	$m_{i_{\text{K}}}$	$c_{NSJM_J m_{i_{\text{Na}}} m_{i_{\text{K}}}}^f$
-1	-3/2	0	-0.149
-1	-1/2	-1	0.447
-1	1/2	-2	-0.291
-1	3/2	-3	-0.154
0	-3/2	-1	-0.194
0	-1/2	-2	-0.236
0	1/2	-3	0.156
0	3/2	-4	0.270
1	-3/2	-2	0.631
1	-1/2	-3	-0.266
1	1/2	-4	-0.103

D. EXCITED STATE AND COUPLING STRENGTH

The hyperfine structures of the excited states have been discussed in details in Ref [S5, S6]. The excited state

is a combination of a mixture of the electronic excited states $B^1\Pi$ $|v = 12, J = 1\rangle$ and $c^3\Sigma$ $|v = 35, J = 1\rangle$, and thus can be expressed as $|\psi_e\rangle = |\psi_{B^1\Pi}\rangle + |\psi_{c^3\Sigma}\rangle$.

The triplet component $|\psi_{c^3\Sigma}\rangle$ accounts for the coupling between the Feshbach state and excited state. The good quantum numbers are $N' = 1, S' = 1$ and $J' = 1$, and thus $|\psi_{c^3\Sigma}\rangle$ can be expanded in the uncoupled basis $|N'S'J'M'_J m'_{i_{\text{Na}}} m'_{i_{\text{K}}}\rangle$. The hyperfine and Zeeman interactions for $c^3\Sigma$ state are described by

$$H^c = a_{\text{Na}}^e \mathbf{i}_{\text{Na}} \cdot \mathbf{S} + a_{\text{K}}^e \mathbf{i}_{\text{K}} \cdot \mathbf{S} + g_s \mu_B B_z \quad (\text{S11})$$

The singlet component $|\psi_{B^1\Pi}\rangle$ is responsible for the coupling between the excited state and the ground state. The good quantum numbers are $\Lambda' = 1, \Sigma' = 0, \Omega' = 1$, and $J' = 1$, and thus $|\psi_{B^1\Pi}\rangle$ can be expanded in the uncoupled basis $|J'\Omega'M'_J m'_{i_{\text{Na}}} m'_{i_{\text{K}}}\rangle$. The $B^1\Pi$ state has negligible hyperfine interaction and only the Zeeman interaction is important, which is described by $\langle J'M'_J | H^B | J'M'_J \rangle = \mu_B M'_J B_z / (J'(J' + 1))$. The $B^1\Pi$ and $c^3\Sigma$ states are mixed due to the spin-orbit coupling. The energy and the wave function of the hyperfine levels of the excited states are obtained by diagonalizing the coupled Hamiltonian.

The triplet component of the wave function of the hyperfine levels of the excited state can be expressed as

$$|\psi_{c^3\Sigma}\rangle \propto \sum_{M'_J m'_{i_{\text{Na}}} m'_{i_{\text{K}}}} c_{N'S'J'M'_J m'_{i_{\text{Na}}} m'_{i_{\text{K}}}}^e |N'S'J'M'_J m'_{i_{\text{Na}}} m'_{i_{\text{K}}}\rangle. \quad (\text{S12})$$

Therefore the coupling strength between the excited state and the Feshbach state for the π -polarized pump light can be expressed as [S7]

$$\begin{aligned} \Omega_{ef} &\propto \langle \psi_{c^3\Sigma} | d_0 | \psi_f \rangle \\ &\propto \sum_{M'_J m'_{i_{\text{Na}}} m'_{i_{\text{K}}}} c_{N'S'J'M'_J m'_{i_{\text{Na}}} m'_{i_{\text{K}}}}^e c_{NSJM_J m_{i_{\text{Na}}} m_{i_{\text{K}}}}^f \langle N'S'J'M'_J | d_0 | NSJM_J \rangle \delta_{m'_{i_{\text{Na}}} m_{i_{\text{Na}}}} \delta_{m'_{i_{\text{K}}} m_{i_{\text{K}}}} \\ &\propto \sum_{M_J m_{i_{\text{Na}}} m_{i_{\text{K}}}} c_{N'S'J'M_J m_{i_{\text{Na}}} m_{i_{\text{K}}}}^e c_{NSJM_J m_{i_{\text{Na}}} m_{i_{\text{K}}}}^f (-1)^{J'-M_J} \begin{pmatrix} J' & 1 & J \\ M_J & 0 & -M_J \end{pmatrix}. \end{aligned} \quad (\text{S13})$$

The singlet component of the wave function can be

expressed as

$$|\psi_{B^1\Pi}\rangle \propto \sum_{M'_J m'_{i_{\text{Na}}} m'_{i_{\text{K}}}} c_{J'\Omega'M'_J m'_{i_{\text{Na}}} m'_{i_{\text{K}}}}^e |J'\Omega'M'_J m'_{i_{\text{Na}}} m'_{i_{\text{K}}}\rangle. \quad (\text{S14})$$

Therefore the coupling strength between the excited state and the ground state $|\psi_g\rangle = |NSJM_J m_{i_{Na}} m_{i_K}\rangle$ for the

π -polarized Stokes light is described as [S7]

$$\begin{aligned} \Omega_{eg} &\propto \langle \psi_{B^1\Pi} | d_0 | \psi_g \rangle \\ &\propto \sum_{M'_J m'_{i_{Na}} m'_{i_K}} c_{J'\Omega' M'_J m'_{i_{Na}} m'_{i_K}}^e \langle J'\Omega' M'_J | d_0 | NSJM_J \rangle \delta_{m'_{i_{Na}} m_{i_{Na}}} \delta_{m'_{i_K} m_{i_K}} \\ &\propto c_{J'\Omega' M_J m_{i_{Na}} m_{i_K}}^e (-1)^{J'-M_J} \begin{pmatrix} J' & 1 & J \\ M_J & 0 & -M_J \end{pmatrix} \end{aligned} \quad (\text{S15})$$

The relative coupling strengths listed in Table S1 are calculated using Eqs. (S13) and (S15).

- [S1] J. Aldegunde and J. M. Hutson, Phys. Rev. A **96**, 042506 (2017).
 [S2] I. Temelkov, H. Knöckel, A. Pashov, E. Tiemann, Phys. Rev. A **91**, 032512 (2015).

- [S3] M.-J. Zhu, H. Yang, L. Liu, D.-C. Zhang, Y.-X. Liu, J. Nue, J. Rui, B. Zhao, J.-W. Pan, and E. Tiemann, Phys. Rev. A **96**, 062705 (2017).
 [S4] B. R. Johnson, J. Chem. Phys. **69**, 4678 (1978).
 [S5] J. W. Park, S. A. Will, and M. W. Zwierlein, New J. Phys. **17**, 075016, (2015).
 [S6] K. Ishikawa, T. Kumauchi, M. Baba, and H. Katô, J. Chem. Phys. **96**, 6423 (1992).
 [S7] J. M. Brown and A. Carrington, *Rotational Spectroscopy of Diatomic Molecules*, Cambridge University Press, New York (2003).